Optimal operational strategy for an offgrid hybrid hydrogen/electricity refueling station powered by solar photovoltaics

Xiao Xu [a], Weihao Hu [a,*], Di Cao [a], Qi Huang [a], Wen Liu [b], Mark Z. Jacobson [c], Zhe Chen [d]

[a] School of Mechanical and Electrical Engineering, University of Electronic Science and Technology of China, Chengdu, China
[b] Copernicus Institute of Sustainable Development, Utrecht University, Princetonlaan 8a, 3584 CB, Utrecht, the Netherlands
[c] Department of Civil and Environmental Engineering, Stanford University, USA
[d] Department of Energy Technology, Aalborg University, Pontoppidanstraede 111, Aalborg, Denmark

HIGHLIGHTS

- A novel concept of a hybrid hydrogen/electricity refueling station is proposed.
- The uncertainties are considered and their potential risk is quantified.
- The optimal strategy is obtained by reformulating the problem into a MILP model.

ARTICLE INFO

ABSTRACT

This study introduces a novel concept to provide both electric charging and hydrogen refueling at the same location. A hybrid hydrogen/electricity refueling station (HERS) powered only by solar photovoltaics in a remote area without access to the electrical grid is proposed. This station provides electricity for battery electric vehicles (BEVs) and simultaneously produces hydrogen for hydrogen fuel cell vehicles (HFCVs). Owing to the variability of PV power output and electricity price, electricity and hydrogen demands, this study investigates a possible operational strategy for the offgrid HERS. The objective is to propose optimal operational strategies for such a station to maximize profits by selling electricity and hydrogen to owners of both BEVs and HFCVs. Failure to supply electricity and hydrogen is treated as a penalty in the target function. The scenario-based stochastic method is adopted for this uncertainty modeling, and the conditional value-at-risk is also considered for evaluating the financial risks. The results reveal that 1) the proposed HERS can simultaneously supply the demands of the BEVs and HFCVs and 2) the behavior of HERS (providing energy to BEVs or HFCVs) is determined by several major factors, namely, electricity and hydrogen prices, and the penalty coefficients.

1. Introduction

With the rapid development of the world economy and population, demand rates for fossil fuel depletion have increased dramatically during the 21st century, increasing the risk of energy instability worldwide [1]. Statistics from BP Energy Outlook 2016 [2] and BP Statistical Review of World Energy 2016 [3] show that the global oil consumption increased by 1.9 million barrels per day, approximately two-thirds of which was caused by the transportation sector. The increased use of internal combustion engines for transportation is one of the main causes of environmental pollution [4]. Thus, the use of battery electric vehicles (BEVs) and hydrogen fuel cell vehicles (HFCVs) has attracted much

attention as an alternative to fossil fuel vehicles (FFVs). BEVs and HFCVs can reduce the emissions of air pollutants and greenhouse gases significantly compared to FFVs [5,6]. Energy for BEVs and HFCVs can come directly or indirectly from renewable energy sources (e.g., photovoltaic or wind turbines) without producing pollution. There are many types of fully or partially powered electric vehicles worldwide, including pure electric vehicles, hybrid electric vehicles, and plug-in hybrid electric vehicles. Such vehicles are all more environmentally friendly and energy efficient than FFVs [7]. In recent years, HFCVs have been produced by several vehicle manufacturers including Nissan Motor Corporation, Toyota Motor Corporation, and Fiat Chrysler Automobiles [6]. However, the transition from FFVs to BEVs and HFCVs depends on the wide availability of electric charging stations and hydrogen refueling stations.

Nomenclature

A. Abbreviation

BEVs	Battery Electric Vehicles
CVaR	Conditional Value at Risk
ESSs	Energy Storage Systems
FFVs	Fossil-Fueled Vehicles
HERS	Hydrogen/Electricity Refueling Station
HFCVs	Hydrogen-Fuel Cell Vehicles
HRS	Hydrogen Refueling Station
HST	Hydrogen Storage Tank
LCOH	Levelized Cost of Hydrogen
MILP	Mixed-Integer Linear Programming
PEM	Proton Exchange Membrane
PV	Photovoltaic
RESs	Renewable Energy Sources

B. Index

s	Scenario index
t	Time index
Ω_s	Total scenarios
T	Total simulation time

C. Parameters

EP_t	Electricity price at time t ($/kWh)
e^{BEV}	Penalty coefficient caused by the non-supplied demand of BEVs ($/kWh)
e^{HFCV}	Penalty coefficient caused by the non-supplied demand of HFCVs ($/m^3)
F	Faraday constant (C mol^{-1})
$G_{t,s}^T$	Solar radiation at time t and scenario s (W/m^2)
G^{REF}	Solar radiation at reference conditions (1000 W/m^2)
HP	Hydrogen price ($/m^3)
k^P	Temperature coefficient of the peak power (1/^{o}C)
$M_{t,s}^{ELE}$	Amount of hydrogen produced by the electrolyzer (mol h^{-1})
$M_{t,s}^{FC}$	Amount of hydrogen consumed by the fuel cell (mol h^{-1})
$P_{t,s}^{PV}$	PV power output at time t and scenario s (kW)
$P^{PV,max}$	The size of the PV power station (kW)
$P^{ELE,min}$	Minimum electrolyzer power (kW)
$P^{ELE,max}$	Maximum electrolyzer power (kW)
$P^{FC,min}$	Minimum fuel cell power (kW)
$P^{FC,max}$	Maximum fuel cell power (kW)
P^{TANK}	Hydrogen storage tank pressure (Mpa)
$P_{t,s}^{BEV}$	Power demand of BEVs at time t and scenario s (kWh)
R	Gas constant (Mpa (mol K)$^{-1}$)
R_{HERS}	The expected profits of HERS ($)
T^{TANK}	The temperature of the hydrogen tanks (K)
$T_{t,s}^{AMB}$	Ambient temperature at time t and scenario s (^{o}C)
$T_{t,s}^C$	PV module temperature at time t and scenario s (^{o}C)
T^{REF}	PV module temperature at the reference condition (^{o}C)
ΔT	Time constant
V^{ELE}	The value of the operational voltage (V)
$V_{t,s}^{TANK}, V_{t-1,s}^{TANK}$	The hydrogen stored in the hydrogen storage tank at time t and scenario s and at time t-1 and scenario s (m^3)
$V_{t,s}^{HFCV}$	The hydrogen demand of HFCVs at time t and scenario s (m^3)
$V^{TANK,min}$	Minimum volume of the hydrogen storage tank (m^3)
$V^{TANK,max}$	Maximum volume of the hydrogen storage tank (m^3)
η^{COM}	The efficiency of the compressor (%)
η^{FC}	The efficiency of the fuel cell (%)
$\eta^{PV,conv}$	The converter efficiency between the PV and the electrolyzer (%)
$\eta^{FC,conv}$	The converter efficiency between fuel cell and BEV (%)
ξ_{CVaR}	CVaR with a confidential level α
α	Confidential level of CVaR (%)
ρ_s	Probability of occurrence at scenario s

D. Decision variables

$P_{t,s}^{FC\_BEV}$	Power supplied to the BEVs generated from the fuel cell (kW)
$P_{t,s}^{RE\_BEV}$	Power supplied to the BEVs from the PV power station (kW)
$P_{t,s}^{RE\_ELE}$	Power supplied by the PV power station to the electrolyzer (kW)
$U_{t,s}^{ELE}$	Binary variable used to control the electrolyzer behaviors
$U_{t,s}^{FC}$	Binary variable used to control the fuel cell behaviors
$V_{t,s}^{TANK\_HFCV}$	Power supplied to the HFCVs from the hydrogen storage tank (m^3)
ζ_α, χ_s	Auxiliary variables for calculating CVaR

For a truly clean hydrogen economy, hydrogen for HFCVs must be produced from renewable electricity [8]. Such hydrogen is referred to as green hydrogen.

Unlike HFCVs, BEVs can be electrically charged directly without energy conversion. Currently, there are different types of batteries available, including lead-acid, sodium-ion, and nickel- and lithium-ion batteries [9]. Among these battery technologies, lithium-ion batteries are currently the most popular choice for BEVs because of their excellent characteristics, e.g., high specific energy and power, and long lifetime. Various types of BEV charging stations have been introduced in the literature [10]. Currently, most of them use either grid electricity or PV power with a grid backup. The design and analysis of a BEV charging station where the electricity comes from PV, are investigated in Refs. [11–13]. The mutual benefit of charging a plug-in hybrid BEV with PV is highlighted in Ref. [14]. The main disadvantage of charging BEVs with PV alone is the intermittency of PV generation. To overcome this disadvantage, charging stations are usually connected to the grid. Additionally, an increasing number of them are being connected to energy storage systems (ESSs) [15,16]. ESSs are charged when there is a surplus of PV power. Subsequently, the stored electricity is used to charge BEVs when PV power is insufficient. Three different methods of charging/discharging the local storage are compared and analyzed in Ref. [17] and the results indicate that a sigmoid function is the best strategy to manage storage behavior. In this work, BEVs are charged with PV power and the storage device is also considered to reduce the effects of PV intermittency.

HFCVs are powered by hydrogen and can be refueled at a hydrogen refueling station (HRS). Hydrogen (H_2) is a naturally occurring molecule in the air; however, it can also be synthetically formed from water (H_2O), methane (CH_4), biomass, or coal [18–20]. Several common methods of hydrogen production include electrolysis; steam reforming of natural gas, methanol, and gasoline; and coal gasification [18,19,21]. Among these, water electrolysis has the potential to emit zero air pollutants and greenhouse gases if the electricity used for it comes from a clean and renewable energy source (RES) [18,19,22,23]. Electrolysis produces hydrogen in capacities varying from small amounts (cm^3/min) to large amounts (m^3/h), and its efficiency is usually over 70% [24]. Hydrogen produced from electrolysis is called electrolytic hydrogen.

Electrolytic hydrogen can either be produced far from a refueling station and sent by pipelines to the refueling station or it can be produced at a refueling station using electricity transmitted to or produced at the refueling station. [22, Supplemental Information, Section S4] proposed the production of hydrogen at local refueling stations using transmitted electricity to avoid the need for hydrogen pipelines. Electricity from photovoltaics (PVs) located at the refueling station can also be used to produce hydrogen. Such a system is most advantageous in remote locations, as they are far from any electrical transmission grid. Once supported by electricity storage systems such as batteries or stationary hydrogen fuel cell storage systems that generate electricity on demand, HRS systems can become more independent of the electricity grid. Several studies have investigated the design and operation of hydrogen production systems based on renewable energy resources [25–27]. Based on a techno-economic analysis, a wind-powered HRS with a 200 HFCVs refueling capacity is analyzed in Ref. [27]. The results indicate that the levelized cost of hydrogen (LCOH) varies from $5.18/kg H$_2$ to $9.62/kg H$_2$. The technical and economic potential of an on-grid HRS powered by a hybrid wind-solar system is investigated in Ref. [28], and the LCOH is €10.3/kg, which is more expensive than a wind-powered HRS. The technical potential of hydrogen production powered by a hybrid energy system including solar, wind, geothermal, and hydroelectric energy is investigated in Ref. [29]. The results show that PV power contributes the most to hydrogen production.

In this work, an autonomous hybrid hydrogen refueling station for HFCVs/electricity for BEVs powered by PV power and storage is proposed and modeled for a remote off-grid area. The proposed offgrid hybrid hydrogen/electricity refueling station, which consists of a PV power station, electrolyzer, compressor, hydrogen storage tank, and stationary hydrogen fuel cell storage system, can simultaneously provide hydrogen to BEVs and power to HFCVs. The hydrogen demand of HFCVs is met by the hydrogen in the hydrogen storage tank. The electricity required for the BEVs can come directly from either the PV panels or from the stationary hydrogen fuel cell storage system. Notably, all the electricity for the system originates from the PVs. With the proposed model, this work investigates the operational strategy of HERS considering the variability of PV power output, electricity demand variability by BEVs, and hydrogen demand variability by HFCVs. Few papers have analyzed the operation of an HRS powered by renewable electricity [30]. To address the inherent uncertainties mentioned, a scenario-based stochastic optimization method is employed to schedule HERS. This method has been widely used for operational problems [31,32]. In addition, the conditional value at risk (CVaR), as a risk measure, is applied to control the risk of these uncertainties [33]. CVaR is introduced based on the value at risk (VaR), which indicates that the loss exceeds the expected loss of VaR at a given confidence level. A more detailed description of the CVaR can be found in Ref. [34].

The main contributions of this paper can be summarized as follows:

1. An autonomous hybrid hydrogen/electricity refueling station, powered by solar photovoltaics and capable of supporting the energy demand of both BEVs and HFCVs simultaneously, is proposed. To the best of the authors' knowledge, this concept has not been previously reported in the literature.
2. This work considers the variability of PV power output, BEV electricity demand, and HFCVs hydrogen demand by using a scenario-based stochastic optimization method to investigate the operational problem of the proposed HERS to maximize profits. Moreover, the CVaR methodology is applied to quantify the potential risk of the operational problem.
3. Simple models are constructed in this work to represent the electrolyzer, hydrogen storage tank, and fuel cell. This allows us to reformulate the operational problem into a mixed-integer linear programming (MILP) problem. Based on the developed MILP problem, the global optimal operational strategy is obtained using Gurobi.
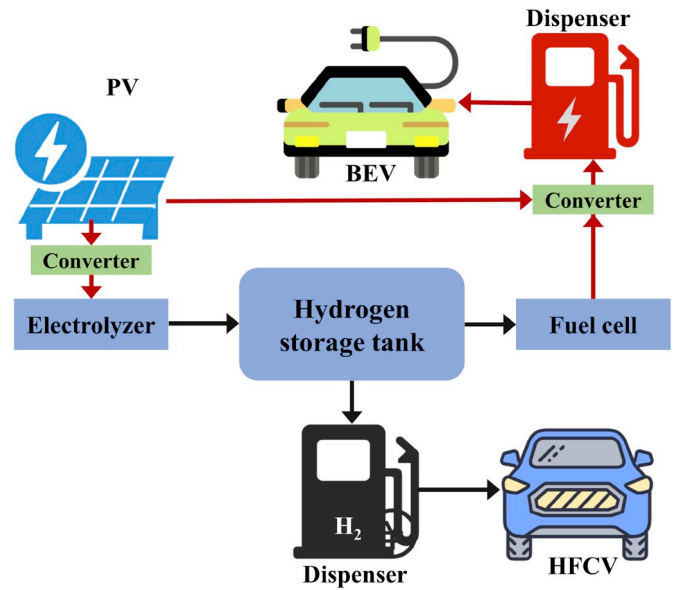

Fig. 1. Schematic diagram of an autonomous hybrid hydrogen refueling/power charging station powered by a PV power station.

The following sections are organized as follows. Section 2 describes the PV output model and the hydrogen production system model; moreover, it formulates a MILP problem. Section 3 provides a case study to validate the proposed HERS. Finally, Section 4 is the conclusion.

2. Models and problem formulation

2.1. Models

In this work, an autonomous hybrid hydrogen/electricity refueling station powered by a PV power station is proposed. The schematic diagram of the proposed system, consisting of a PV power station, electrolyzer, hydrogen storage tank (HST), fuel cell, and two dispensers, is shown in Fig. 1. The red and black arrows in Fig. 1 represent the power and hydrogen flow, respectively. The power generated by the PV power station can be divided into two parts: one part is directly supplied to electric vehicles when there is adequate PV power and the other part is used to produce hydrogen by using an electrolyzer. Afterward, the produced hydrogen is compressed into a hydrogen storage tank via a compressor. The hydrogen storage tank supplies hydrogen to the hydrogen-fueled vehicles and fuel cell to generate electricity for electric vehicles. The fuel cell works to generate electricity when the PV power is insufficient. All the energy of HERS comes from the PV power station which can help to achieve zero-emissions. Therefore, it is clear that HERS are especially important for the spread of BEVs and HFCVs. This section presents the models of each component of the proposed HERS.

2.1.1. PV power station

Recently, the popularity of RESs, e.g., solar power, has increased significantly. The uncertainty of PV power output is a challenge for the power system. To reduce the negative impact of the uncertainty and intermittency of PV power output, it is necessary to forecast and estimate solar radiation. Many studies have estimated solar radiation based on historical data. The uncertain solar radiation can be modeled by the probability density function to forecast PV power outputs. To produce solar radiation scenarios, the normal distribution function can be employed. The available power generated by the PV power station in each period and scenario can be formulated as [35]:

$$P_{t,s}^{PV} = \eta^{PV,conv} P^{PV,\max} \frac{G_{t,s}^T}{G^{REF}} \left[1 + k^P \left(T_{t,s}^C - T^{REF} \right) \right] \tag{1}$$

$$T_{t,s}^C = T_{t,s}^{AMB} + \left(0.0256 \times G_{t,s}^T\right) \qquad (2)$$

where $P^{PV,\max}$ represents the size of the PV power station. $\eta^{PV,conv}$ represents the converter efficiency between the PV and the electrolyzer. $P^{PV,\max}$ represents the size of the PV power station. $G_{t,s}^T$ represents the solar radiation at time t and scenario s. G^{REF} represents the solar radiation at reference conditions. k^P represents the temperature coefficient of the peak power. $T_{t,s}^C$ represents the PV module temperature at time t and scenario s. T^{REF} represents the PV module temperature at the reference condition. Finally, $T_{t,s}^{AMB}$ represents the ambient temperature at time t and scenario s.

2.1.2. Hydrogen production system modeling

Many hydrogen production systems models can be found in the literature [36–38]. However, some of these models are too complex, have incomplete parameters, or use the off-the-shelf tool (HOMER). To address these problems, this paper introduces a relatively simple hydrogen production system model with detailed parameters. The model can be used for its design and operational problems. The hydrogen production system includes an electrolyzer, hydrogen storage tank, and fuel cell. Notably, the hydrogen production system also contains other components such as a compressor and a cooling system. When PV power is available, it can be converted into hydrogen through an electrolyzer and stored in a hydrogen storage tank. Consequently, the stored hydrogen can be supplied to satisfy the demands of HFCVs and fuel cells to generate electricity to meet the demands of BEVs. Detailed models of the electrolyzer, hydrogen storage tank, and fuel cell are presented below.

2.1.2.1. Electrolyzer.
The Proton Exchange Membrane (PEM) is selected in this work as the electrolyzer [39], which is a relatively new technology compared to the alkaline electrolyzer. However, its construction is simpler than that of the alkaline electrolyzer [40]. Theoretically, the efficiency of the PEM electrolyzer can reach up to 94% under a higher heating value [41]; however, the best efficiency so far is over 85% [42, 43]. In the electrolysis process, the electrolyzer breaks down water into hydrogen and oxygen. This process can be expressed as:

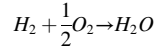$$H_2O + \text{electricity} \rightarrow H_2 + \frac{1}{2}O_2$$
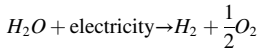
The lower and upper limits of the power consumed by the electrolyzer are given below (Eq. (4)). The amount of hydrogen produced by the PEM electrolyzer may be formulated as follows:

$$M_{t,s}^{ELE} = \eta^{COM} \frac{P_{t,s}^{RE-ELE} \Delta T}{2 V^{REF} F} \qquad (3)$$

$$P^{ELE,\min} U_{t,s}^{ELE} \leq P_{t,s}^{RE-ELE} \leq P^{ELE,\max} U_{t,s}^{ELE} \qquad (4)$$

where $M_{t,s}^{ELE}$ represents the amount of hydrogen produced by the electrolyzer. η^{COM} represents the efficiency of the compressor. $P_{t,s}^{RE-ELE}$ represents the power supplied by the PV power station to the electrolyzer. ΔT represents the time constant. V^{ELE} is the value of the operational voltage. F is the faraday constant. $P^{ELE,\min}$ and $P^{ELE,\max}$ represent the minimum and maximum electrolyzer power, respectively. Finally, $U_{t,s}^{ELE}$ represents the binary variable used to control the electrolyzer behavior.

2.1.2.2. Fuel cell.
Fuel cells generate electricity to satisfy the demand of BEVs by consuming the stored hydrogen. The PEM fuel cell performs well at startup and shutdown. Therefore, it may be the most suitable choice among all types of fuel cells [44]. The chemical reaction occurring in the PEM fuel cell is as follows:

$$H_2 + \frac{1}{2}O_2 \rightarrow H_2O$$

The lower and upper limits of the stored hydrogen consumed by the PEM fuel cell are given below (Eq. (6)). The amount of hydrogen produced by the PEM electrolyzer may be formulated as follows:

$$M_{t,s}^{FC} = \frac{P_{t,s}^{FC-BEV} \Delta T}{2.96 \eta^{FC} \eta^{FC,conv} F} \qquad (5)$$

$$P^{FC,\min} U_{t,s}^{FC} \leq P_{t,s}^{FC} \leq P^{FC,\max} U_{t,s}^{FC} \qquad (6)$$

where $M_{t,s}^{FC}$ represents the amount of hydrogen consumed by the fuel cell. $P_{t,s}^{FC-BEV}$ represents the power supplied to the BEVs from the PV power station. η^{FC} represents the efficiency of the fuel cell. $\eta^{FC,conv}$ represents the converter efficiency between the fuel cell and BEV. $P^{FC,\min}$ and $P^{FC,\max}$ represent the minimum and maximum fuel cell power, respectively. Finally, $U_{t,s}^{FC}$ represents the binary variable used to control the fuel cell behavior.

2.1.2.3. Hydrogen storage tank.
The hydrogen storage tank can store the hydrogen produced with the available power generated by the PV power station. Afterward, the stored hydrogen can be used to meet the demand of HFCVs and BEVs. It is assumed that no leakage occurs in the hydrogen storage tank [40]. The initial amount of hydrogen in the hydrogen storage tank is assumed to be 50% of the tank size in this work. Notably, the electrolyzer and fuel cell cannot operate simultaneously. However, the hydrogen storage tank can supply hydrogen to the HFCVs and fuel cells simultaneously. Eq. (7) can manage the electrolyzer and fuel cell behavior to prevent them from working at the same time. The dynamic equation of hydrogen volume in the HST is given in Eq. (8). Finally, the minimum and maximum limits of HST are given in Eq. (9).

$$U_{t,s}^{ELE} + U_{t,s}^{FC} \leq 1 \qquad (7)$$

$$V_{t,s}^{TANK} = V_{t-1,s}^{TANK} + \frac{R T^{TANK}}{P^{TANK}} \left(M_{t,s}^{ELE} - M_{t,s}^{FC}\right) - V_{t-1,s}^{TANK-HFCV} \qquad (8)$$

$$V^{TANK,\min} \leq V_{t,s}^{TANK} \leq V^{TANK,\max} \qquad (9)$$

where $V_{t,s}^{TANK}$ and $V_{t-1,s}^{TANK}$ represent the hydrogen stored in the hydrogen storage tank at both time t and scenario s as well as at time t-1 and scenario s. R represents the gas constant. T^{TANK} represents the temperature of the hydrogen tanks. P^{TANK} represents the hydrogen storage tank pressure. $V_{t-1,s}^{TANK-HFCV}$ represents the power supplied to the HFCVs from the hydrogen storage tank at time t-1 and scenario s. $V^{TANK,\min}$ and $V^{TANK,\max}$ represent the minimum and maximum volume of the hydrogen storage tank, respectively.

2.1.3. Conditional value at risk

In this work, the CVaR is used to control the financial risks caused by the uncertainties of PV power outputs and the behavior of BEVs and HFCVs. CVaR is coherent and can preserve the convexity of the optimization models. Thus, the optimization problem is manageable. CVaR can be calculated using the following equations [45].

$$\xi_{CVaR} = \max \left(\zeta_\alpha - \frac{1}{1-\alpha} \sum_{s=1}^{\Omega_s} \rho_s \chi_s\right) \qquad (10)$$

$$\text{s.t. } \chi_s \geq \zeta_\alpha - R_s, \forall s \qquad (11)$$

$$\chi_s \geq 0, \forall s \qquad (12)$$

where ξ_{CVaR} represents the CVaR with a confidential level of α. ζ_α and χ_s are auxiliary variables. α is the confidential level of CVaR. Finally, ρ_s

represents the probability of occurrence at scenario *s*. In the above equations, if the value of expected revenue, R_s, in scenario s is greater than ζ_α, χ_s is considered to be zero. Otherwise, χ_s is equal to the difference between R_s and ζ_α. Therefore, the optimal expected revenue is equal to ζ_α under the confidence degree of α[46].

2.2. Problem formulation

This work proposes an autonomous HERS powered by a PV power station to provide energy for BEVs and HFCVs in a remote area. The HERS retailer sells hydrogen to HFCVs and electricity to BEVs to obtain maximum profits. However, the demand for BEVs and HFCVs may not be completely satisfied during the day as the HRPCS is off-grid and PV power production, as well as the demand for BEVs and HFCVs, are uncertain. Eq. (13) shows the objective of the work, which is to maximize the expected revenue considering the CVaR risk. The first term of Eq. (13) is the expected revenue of HERS, and it is calculated by Eq. (14). The second term of Eq. (13) is the calculation of the CVaR risk, which is multiplied by a weighting factor *β* (e.g., the risk preference of decision-makers). A higher *β* value indicates that a decision-maker can only tolerate low financial risks. Eq. (14) contains four parts, which are the revenue generated from the sale of power to BEVs (first term) and from the sale of hydrogen to HFCVs (second term), the penalty caused by the non-supplied demand of BEVs (third term) and the penalty caused by the non-supplied demand of HFCVs (last term). The sum of the power supplied to the BEVs and electrolyzer is limited by the PV power output, which is given in Eq. (15). Eq. (16) shows that the power delivered to BEVs should be constrained by the demand of BEVs. Similarly, the constraint on the demand of HFCVs is given in Eq. (17). Eqs. (18) and (19) are formulated based on Eqs. (11) and (12), which are used to estimate financial risks. The other constraints are summarized in Eq. (20) and the detailed description of these constraints is presented above

$$\max R_{HERS} + \beta \left[\zeta_\alpha - \frac{1}{1-\alpha} \cdot \sum_{s=1}^{\Omega_S} (\rho_s \chi_s) \right] \tag{13}$$

$$R_{HERS} = \sum_{s=1}^{\Omega_S} \rho_s \sum_{t=1}^{T} \left[\left(P_{t,s}^{RE\_BEV} + P_{t,s}^{FC\_BEV} \right) \cdot EP_t + V_{t,s}^{TANK\_HFCV} \cdot HP \right.$$
$$- e^{BEV} \cdot \left(P_{t,s}^{BEV} - P_{t,s}^{RE\_BEV} - P_{t,s}^{FC\_BEV} \right)$$
$$\left. - e^{HFCV} \cdot \left(V_{t,s}^{HFCV} - V_{t,s}^{TANK\_HFCV} \right) \right] \tag{14}$$

$$0 \le P_{t,s}^{RE\_ELE} + P_{t,s}^{RE\_BEV} \le P_{t,s}^{PV} \tag{15}$$

$$0 \le P_{t,s}^{RE\_BEV} + P_{t,s}^{FC\_BEV} \le P_{t,s}^{BEV} \tag{16}$$

$$0 \le V_{t,s}^{TANK\_HFCV} \le V_{t,s}^{HFCV} \tag{17}$$

$$\chi_s \ge \zeta_\alpha - \sum_{t=1}^{T} \left[\left(P_{t,s}^{RE\_BEV} + P_{t,s}^{FC\_BEV} \right) \cdot EP_t + V_{t,s}^{TANK\_HFCV} \cdot HP \right.$$
$$- e^{BEV} \cdot \left(P_{t,s}^{BEV} - P_{t,s}^{RE\_BEV} - P_{t,s}^{FC\_BEV} \right)$$
$$\left. - e^{HFCV} \cdot \left(V_{t,s}^{HFCV} - V_{t,s}^{TANK\_HFCV} \right) \right], \forall s \tag{18}$$

$$\chi_s \ge 0, \forall s \tag{19}$$

$$\{(1) - (9)\} \tag{20}$$

where EP_t represents the electricity price at time *t*. e^{BEV} represents the penalty coefficient caused by the non-supplied demand of BEVs. e^{HFCV} represents the penalty coefficient caused by the non-supplied demand of HFCVs. *HP* represents the price of hydrogen. $P_{t,s}^{BEV}$ represents the power demand of BEVs at time *t* and scenario *s*. R_{HERS} represents the expected
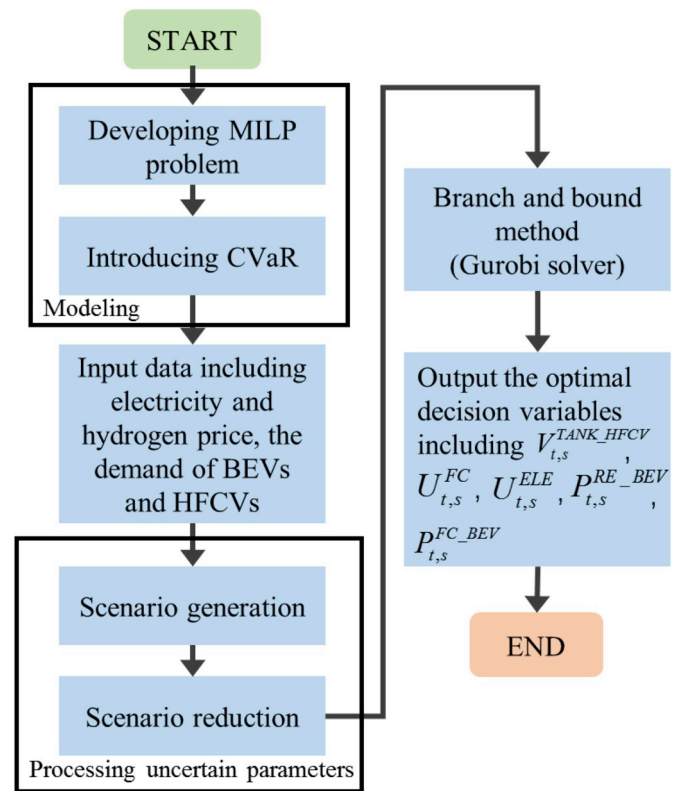

Fig. 2. Optimization process flowchart.

profits of HERS. Finally, $V_{t,s}^{HFCV}$ represents the hydrogen demand of HFCVs at time *t* and scenario *s*.

The flowchart of the entire optimization process is given in Fig. 2. First, the operational problem model considering the CVaR is developed into a MILP problem presented in Eqs. (13)–(20). Furthermore, different uncertainties are considered in this work and the input data, including the PV power output and demand of BEVs and HFCVs, is processed. One thousand scenarios are generated for each uncertain parameter using the scenario generation technique. Afterward, the corresponding number of representative scenarios is reduced to 50 scenarios using the scenario reduction technique. Each of these 50 scenarios can represent the abovementioned three uncertain parameters. Based on the models and scenarios, the optimal operational results containing $P_{t,s}^{FC\_BEV} P_{t,s}^{RE\_BEV}$, $U_{t,s}^{ELE}$, $U_{t,s}^{FC}$, and $V_{t,s}^{TANK\_HFCV}$ can be solved by the Gurobi solver using the branch and bound method. It should be noted that the results obtained are considered globally optimal solutions.

3. Case study

To validate the feasibility of the proposed HERS, a case study is presented below. The operational strategy of the proposed HERS is also investigated to illustrate its features. The operational problem of the proposed HERS is formulated in (13)–(20) as a MILP model that is programed in the Python environment and solved by the Gurobi solver.

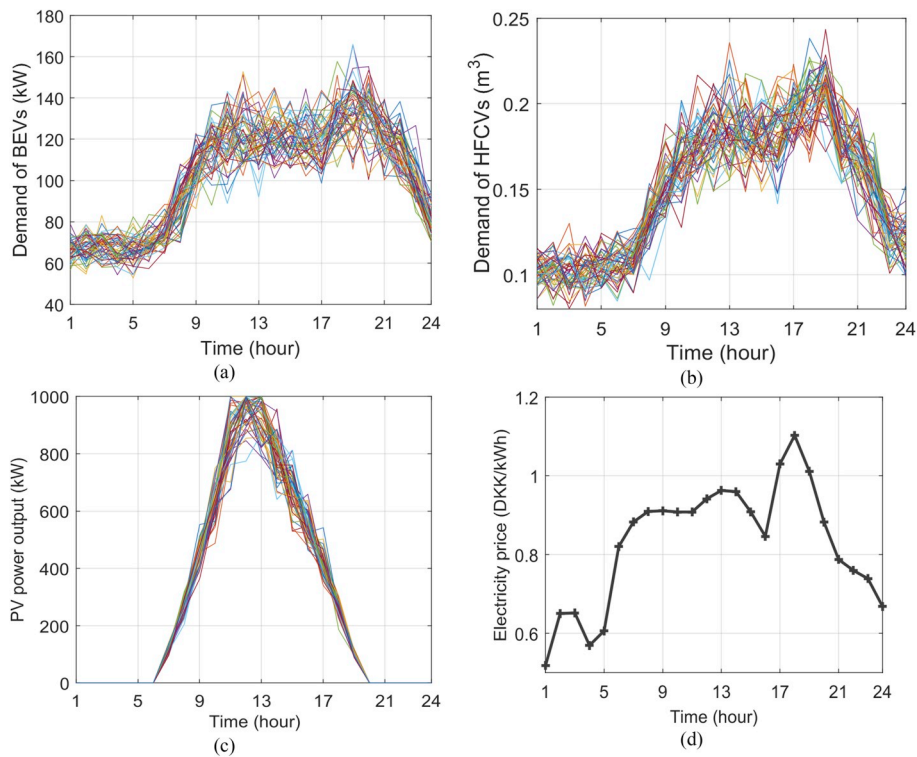**Table 1**
Photovoltaic (PV) power station specifications.

Factors	$P^{PV,max}$	G^{REF}	k^P	T^{REF}	$\eta^{PV.conv}$
Value	1000 kW	1000 W/m²	-3.7×10^{-3} 1/°C	25 °C	95%

Table 2
Hydrogen production system specifications.

Electrolyzer		Hydrogen storage tank	
Factor	Value	Factor	Value
$P^{ELE,min}$, $P^{ELE,max}$	0, 840 kW	$V^{TANK,min}$, $V^{TANK,max}$	0, 7.42 m^3
η^{COM}	95%	R	0.008211 MPa (mol K)$^{-1}$
ΔT	3600	T^{TANK}	298 K
V^{ELE}	2 V	P^{TANK}	20 MPa
F	96485 C mol^{-1}	–	–
Fuel cell		–	–
Factor	**Value**	–	–
$P^{FC,min}$, $P^{FC,max}$	0, 150 kW	–	–
$\eta^{FC,conv}$	95%	–	–
η^{FC}	47%	–	–

3.1. Data

This work investigates the operational problem of the proposed HERS; therefore, the detailed parameters of the PV power station and hydrogen production system are given in Table 1 [35] and Table 2 [37], respectively. Notably, the size of the electrolyzer is greater than that of the fuel cell, as the electrolyzer needs to produce more hydrogen to meet the demand of the HFCVs and fuel cell. To optimize the HERS operational problem, a deterministic prediction is considered and different scenarios are generated to capture the uncertainties of the forecasted parameters, including PV power outputs and the demand of BEVs and HFCVs. The uncertainties of these three parameters are considered to be represented by forecasting errors. In addition, all forecast errors are assumed to follow a normal distribution. For each uncertain parameter, one thousand scenarios are generated using the scenario generation technique [47]. Afterward, the corresponding number of representative scenarios is reduced to 50 scenarios with high probability of occurrence via the scenario reduction technique [48]. In the end, all 50 scenarios are used to represent these three uncertain parameters in the HERS

Fig. 3. Simulation dataset (a) Demand of BEVs in 50 scenarios (b) Demand of HFCVs in 50 scenarios (c) PV power output in 50 scenarios (d) Electricity price.
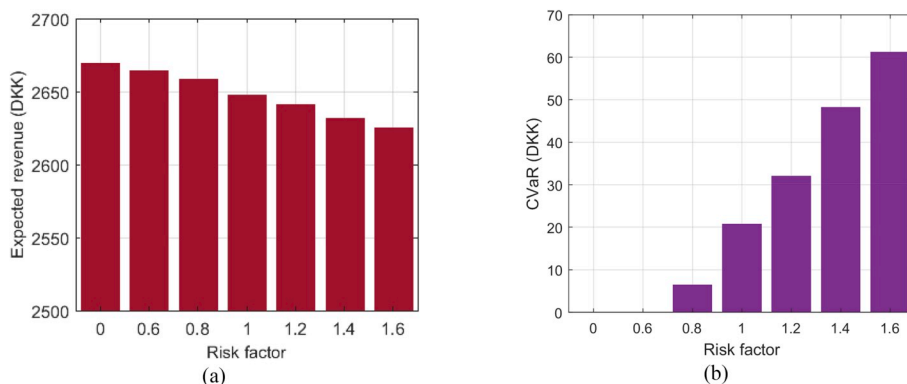
Fig. 4. Results under different risk factors. (a) Expected revenue (b) CVaR values.

Table 3
Value of the expected revenue and CVaR under different risk factors.

Risk factor	0	0.6	0.8	1.0	1.2	1.4	1.6
Expected revenue (DKK)	2670	2665	2659	2648	2642	2632	2626
CVaR (DKK)	0	0	6.51	20.78	32.03	48.22	61.27

operational problem. Fig. 3. (a) and (b) show the demand of BEVs and HFCVs in 50 scenarios, respectively. During the daytime, their demands are high owing to the large traffic flow. Fig. 3. (c) presents the PV power outputs during the day, which is the source of all the energy of BEVs and HFCVs, and the size of the PV power station is set at 1000 kW. In this work, it is assumed that the electricity price in a day is variable (but it can be known one day ahead) and hydrogen price in a day is fixed. The electricity price during the day is shown in Fig. 3. (d). The hydrogen price in a day is assumed to be 0.5 DKK/kWh (9.28×10^{-4} DKK/m^3), which is converted to be consistent with the unit price of electricity for better comparison. The penalty coefficients caused by the BEVs' and HFCVs' non-supplied demand are set at 0.5 DKK/kWh under the same unit. The initial amount of hydrogen in the hydrogen storage tank is assumed to be 50% of the tank size. First, the impact of different risk factors on the CVaR and expected revenue is investigated. Afterward, based on $\beta = 0$, detailed simulation results are presented. HERS, which can store/supply hydrogen to HFCVs, may cause serious accidents owing to safety problems including pipeline failure, reaction with pollutants, low hydrogen purity, wrong operations, etc. [49]. In this work, it is assumed that the station can operate under safe conditions as the research mainly focuses on its benefits considering the uncertainty of PV power output.
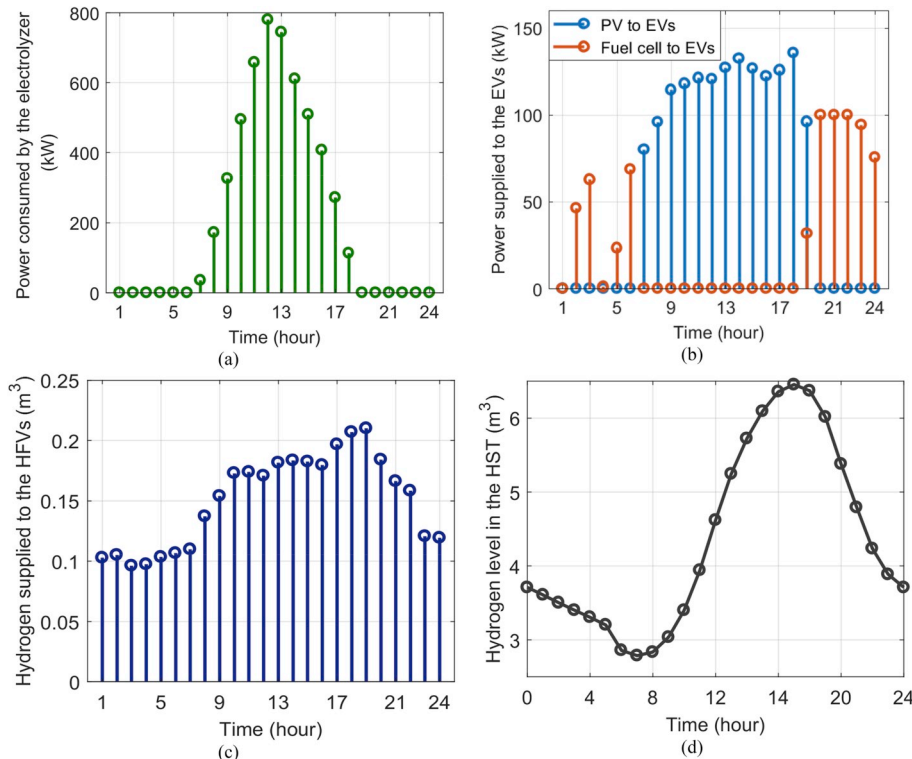
3.2. Results

The effects of various risk factors on the expected revenue and CVaR, with a 95% confidentiality level, are presented in Fig. 4. (a) and (b),

respectively. The risk aversion parameter values are determined by the CVaR with a 95% confidence level ($\alpha = 0.95$), which is approximately equal to the expected revenue of the 5% scenarios with the lowest revenue. As can be seen in the two figures, the measured risk decreases with the increase in the CVaR. The decision-maker must tolerate the higher risk when the risk factor is zero. If the decision-maker becomes more risk-averse as the value of the risk factor β increases, the expected revenue and risk could be lower. Under different risk factors, the operational strategies of the HRPCS are diverse. The expected revenue and CVaR under different risk factors are summarized in Table 3. The below simulation analysis is conducted when the risk factor is zero ($\beta = 0$), which means that the decision-maker aims to maximize expected revenue without considering any financial risk.

The power generated by the PV power station can be used to produce hydrogen via an electrolyzer and be directly supplied to BEVs. The amount of PV power consumed by the electrolyzer is shown in Fig. 5. (a), which is used to produce hydrogen. Notably, the electrolyzer works to produce hydrogen when there is adequate PV power output; otherwise, it does not work. The hydrogen produced can then be supplied to the HFCVs and fuel cells to generate electricity. The demand of BEVs is satisfied by the PV power station and fuel cell. Power supplied to BEVs from the PV power station and the fuel cell is shown in Fig. 5. (b). During the daytime, the power generated by the PV power station can be directly delivered to BEVs without any loss of energy conversion. In the case of no PV power output during the night, the fuel cell operates to generate power to meet the demand of BEVs by consuming the hydrogen stored in the HST. At 1:00, the fuel cell does not work because of the relatively lower electricity price, which can be seen in Fig. 3. (d). At 19:00, all the power generated by the PV power station is supplied to BEVs. In addition, the fuel cell generates part of the electricity for the BEVs by consuming the stored hydrogen because of the relatively higher electricity price.

Fig. 5. (c) gives the volume of hydrogen supplied to HFCVs that is related to the HFCVs' demand. Hydrogen is produced when there is the

Fig. 5. Simulation results (a) PV power consumed by the electrolyzer (b) Power supplied to BEVs from the PV power station and fuel cell (c) Volume of the hydrogen supplied to HFCVs (d) Change in hydrogen level in the HST.
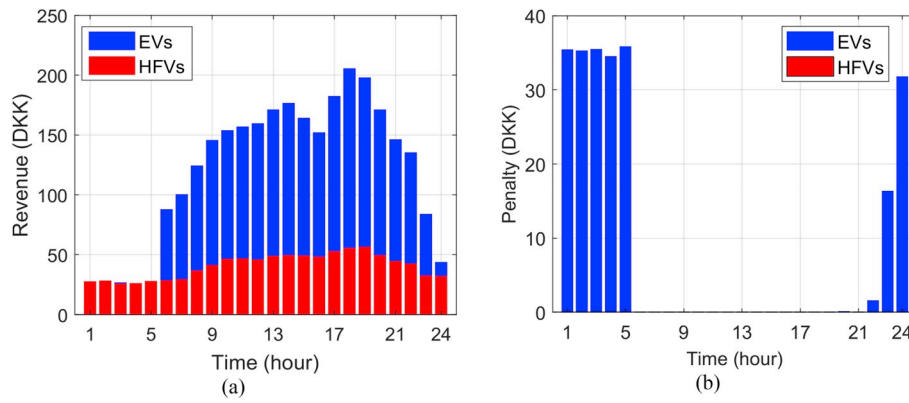
Fig. 6. Simulation results (a) Expected revenue from BEVs and HFCVs (b) Penalty caused by the non-supplied demand of BEVs and HFCVs.
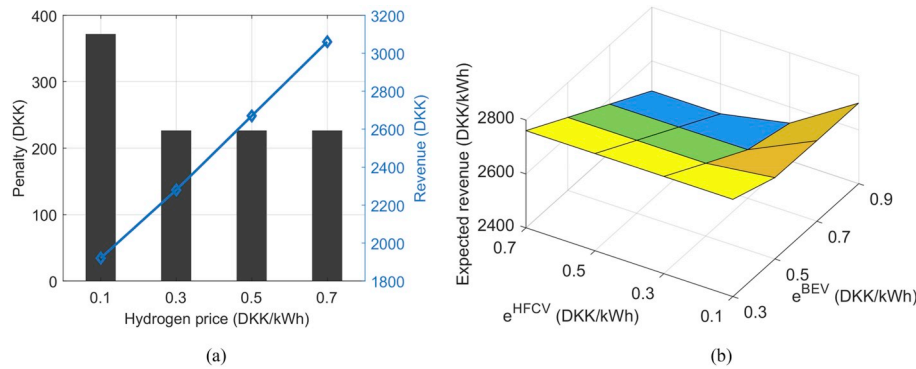

Fig. 7. Sensitivity analysis (a) Penalty and expected revenue under different hydrogen prices (b) Expected revenue under different e^{BEV} and e^{HFCV}

adequate PV power output and then stored in the HST. During the day, hydrogen stored in the HST is continuously supplied to the HFCVs. The change in the level of hydrogen in the HST during the day is shown in Fig. 5. (d), which depends on the consumption of the HFCVs and fuel cells. From 0:00 to 7: 00 and from 15:00 to 24:00, the hydrogen level curve shows a downward trend as the HST is consuming hydrogen without producing it. When there is enough PV power output from 7:00 to 15:00, there is an increase in the hydrogen stored in the HST as the amount of hydrogen produced is far greater than the amount of hydrogen consumed. To meet the hydrogen demand of the next day, it is considered that the hydrogen stored in the HST at the beginning of the day should be equal to that at the end of the day. Therefore, as can be seen in Fig. 5. (d), the hydrogen level at 0:00 is equal to that at 24:00. Based on the above analysis, the importance of HST in satisfying the demand of BEVs and HFCVs is shown.

The aim of this work is to maximize the expected revenue, which is equal to the revenue obtained from selling hydrogen to HFCVs and electricity to BEVs minus the penalty caused by the non-supplied demand of HFCVs and BEVs. Moreover, Fig. 6. (a) shows the expected revenue from BEVs and HFCVs. As shown, HFCVs can bring benefits throughout the day. At 1:00, 2:00, 4:00, and 5:00, no profit can be made from BEVs because of the relatively lower electricity price. The same situation occurs at 3:00, although a small amount of revenue can be obtained. Therefore, the question of how to achieve the highest possible profit from the sale of hydrogen to HFCVs or the sale of electricity to BEVs depends on the price of electricity, price of hydrogen, demand of HFCVs and BEVs, and the efficiency of energy conversion. For an autonomous system, it is difficult to guarantee maximum reliability, i.e., non-supplied demand of BEVs and HFCVs may occur. To reduce the occurrence of such a situation, the penalty caused by the non-supplied demand of BEVs and HFCVs is considered and the results during the day are shown in Fig. 6. (b). Notably, only BEVs lead to a penalty, i.e.,

only the demand of BEVs may not be completely satisfied. Moreover, the non-supplied demand of BEVs occurs at night. This is because the electricity price is relatively low at night and the energy conversion can cause energy loss. Compared to the direct sale of hydrogen to HFCVs, it is not cost-effective to generate electricity for BEVs using fuel cells.

In this paper, the hydrogen price is assumed to be 0.5 DKK/kWh (9.28×10^{-4} DKK/m^3), which is consistent with the unit price of electricity for better comparison. Therefore, the impact of different hydrogen prices on the penalty and expected revenue is analyzed using the DKK/kWh unit, which is shown in Fig. 7. (a). As the hydrogen price increases from 0.1 DKK/kWh to 0.7 DKK/kWh, the blue curve of expected revenue shows an upward trend. The penalty decreases from 371.6 DKK to 226.4 DKK when the hydrogen price increases from 0.1 DKK/kWh to 0.3 DKK/kWh. Afterward, the penalty no longer changes as hydrogen price increases from 0.3 DKK/kWh to 0.7 DKK/kWh because the situation of non-supplied demand of HFCVs cannot occur when hydrogen price is greater than 0.3 DKK/kWh. Thus, hydrogen price being one of the most important parameters, affects the penalty caused by the non-supplied demand of HFCVs. In addition, other important parameters are also investigated. Fig. 7. (b) shows the expected revenue under different penalty coefficients caused by the non-supplied demand of BEVs and HFCVs. Similarly, the unit of e^{HFCV} is converted to be consistent with the unit of e^{BEV} for better comparison. The demand of BEVs is more significant than the demand of HFCVs when e^{BEV} is 0.4 DKK/kWh higher than e^{HFV}. Both parameters are very important to determine the situations of non-supplied demand of BEVs and HFCVs; besides, they affect the expected revenue. Fig. 7. (b) shows that the increase of both values (e^{BEV} and e^{HFCV}) can lead to the reduction of the expected revenue as the penalty of the system will also increase.

Additionally, this work aims to investigate the operational problem of HERS. It is assumed that the size of the PV power station is 1000 kW based on the demand of BEVs and HFCVs. Proper sizing of HERS is
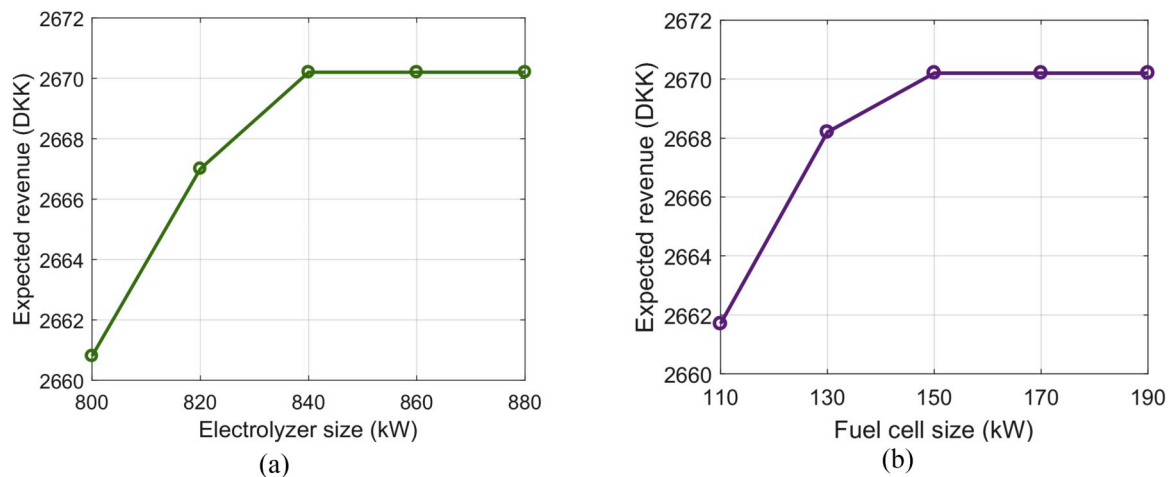
Fig. 8. Expected revenue (a) Under different electrolyzer sizes (b) Under different fuel cell sizes.

important as it can determine the economic benefits of the station. Therefore, the impact of different electrolyzer and fuel cell sizes is investigated. Fig. 8. (a) shows the expected revenue under different electrolyzer sizes with a fixed fuel cell size (150 kW). The expected revenue increases from 2660.8 DKK to 2670.2 DKK when the electrolyzer size increases from 800 kW to 840 kW; therefore, the expected revenue is a constant. Fig. 8. (b) shows the expected revenue under different fuel cell sizes with a fixed electrolyzer size (840 kW). Notably, the expected revenue is unchanged when the fuel cell size reaches 150 kW. Therefore, the 840 kW electrolyzer and 150 kW fuel cell may be the best choice under the given conditions.

4. Conclusion

This work proposes a novel concept of an autonomous hybrid hydrogen/electricity refueling station. This station can simultaneously supply power and hydrogen to BEVs and HFCVs, respectively. When there is enough PV power output, the demand of BEVs can be directly supplied and the electrolyzer works to produce hydrogen. In this way, the stored hydrogen is used to refuel HFCVs. In addition, hydrogen can also be converted into electricity by using fuel cells to charge BEVs. The uncertainties and risks associated with PV power outputs as well as the demand of BEVs and HFCVs are addressed via multiple representative stochastic scenarios. Based on these scenarios, models of the operational problem of the autonomous hybrid hydrogen/electricity refueling station are developed. Subsequently, numerical results are provided to validate the feasibility of the proposed HERS. The proposed HERS is worthy for the promotion of BEVs and HFCVs in the future. If HFCVs do not have the same market impact as BEVs, the sizes of the hydrogen production devices (such as the electrolyzer and hydrogen storage tank) may be smaller. Therefore, HERS can generate more electricity and less hydrogen. Moreover, if BEVs or HFCVs are not economically viable options in the future, hydrogen can be transported to other places to be sold for industrial applications and injected into the natural gas pipeline for profit.

In future works, the design problem of the proposed HERS will be investigated. Finally, safety aspects will be introduced and the relationship between primary and secondary safety features together with the benefits and feasibility of such a station will be analyzed.

Declaration of competing interest

The authors declared that they have no conflicts of interest to this work. We declare that we do not have any commercial or associative interest that represents a conflict of interest in connection with the work submitted.

References

[1] J. Alazemi, J. Andrews, Automotive hydrogen fuelling stations:an international review, Renew. Sustain. Energy Rev. 48 (2015) 483–499.
[2] British Petroleum, BP energy outlook 2016. https://doi.org/10.1017/CBO9781107415324.004, 2016, 53.
[3] British Petroleum, BP statistical review of world, Energy (2016).
[4] Roberto Pili, Alessandro Romagnoli, Kai Kamossa, Andreas Schuster, Hartmut Spliethoff, Christoph Wieland, Organic Rankine Cycles (ORC) for mobile applications – economic feasibility in different transportation sectors, Appl. Energy 204 (2017) 1188–1197.
[5] Lia Kouchachvili, W. Yaïci, E. Entchev, Hybrid battery/supercapacitor energy storage system for the electric vehicles, J. Power Sources 374 (2018) 237–248.
[6] Kriston P. Brooks, Richard P. Pires, Kevin L. Simmons, Development and validation of a slurry model for chemical hydrogen storage in fuel cell vehicle applications, J. Power Sources 271 (2014) 504–515.
[7] Huaqiang Liu, Zhongbao Wei, Weidong He, Jiyun Zhao, Thermal issues about Li-ion batteries and recent progress in battery thermal management systems: a review, Energy Convers. Manag. 150 (2017) 304–330.
[8] Murat Gökçek, Cihangir Kale, Optimal design of a hydrogen refuelling station (HRFS) powered by hybrid power system, Energy Convers. Manag. 161 (2018) 215–224.
[9] H. Budde-Meiwes, J. Drillkens, B. Lunz, J. Muennix, S. Rothgang, J. Kowal, et al., A review of current automotive battery technology and future prospects, Proc. Inst. Mech. Eng. - Part D J. Automob. Eng. 227 (2013) 761–776.
[10] Fathabadi Hassan, Novel wind powered electric vehicle charging station with vehicle-to-grid (V2G) connection capability, Energy Convers. Manag. 136 (2017) 229–239.
[11] G.R. Chandra Mouli, P. Bauer, M. Zeman, System design for a solar powered electric vehicle charging station for workplaces, Appl. Energy 168 (2016) 434–443.
[12] Andrew Meintz, et al., Enabling fast charging-Vehicle considerations, J. Power Sources 367 (2017) 216–227.
[13] P. Nunes, T. Farias, M.C. Brito, Day charging electric vehicles with excess solar electricity for a sustainable energy system, Energy 80 (2015) 263–274.
[14] Denholm Paul, Michael Kuss, M. Robert, Margolis. Co-benefits of large scale plug-in hybrid electric vehicle and solar PV deployment, J. Power Sources 236 (2013) 350–356.
[15] M. Tesfaye, C.C. Castello, Minimization of impact from electric vehicle supply equipment to the electric grid using a dynamically controlled battery bank for peak load shaving, in: 2013 IEEE PES Innov Smart Grid Technol Conf, IEEE, 2013, pp. 1–6.
[16] N. Kawamura, M. Muta, Development of solar charging system for plug-in hybrid electric vehicles and electric vehicles, in: 2012 Int Conf Renew Energy Res Appl, IEEE, 2012, pp. 1–5.
[17] C.C. Castello, T.J. LaClair, L.C. Maxey, Control strategies for electric vehicle (EV) charging using renewables and local storage, in: 2014 IEEE Transp Electrif Conf Expo, IEEE, 2014, pp. 1–7.
[18] M.Z. Jacobson, W.G. Colella, D.M. Golden, Cleaning the air and improving health with hydrogen fuel cell vehicles, Science 308 (2005) 1901–1905.
[19] W.G. Colella, M.Z. Jacobson, D.M. Golden, Switching to a U.S. hydrogen fuel cell vehicle fleet: the resultant change in emissions, energy use, and global warming gases, J. Power Sources 150 (2005) 150–181.

[20] A. Valente, D. Iribarren, J. Dufour, Harmonised life-cycle global warming impact of renewable hydrogen, J. Clean. Prod. 149 (2017) 762–772.

[21] A. Ete, Hydrogen Systems Modelling, Analysis and Optimisation, University of Strathclyde, 2009.

[22] M.Z. Jacobson, Effects of wind-powered hydrogen fuel cell vehicles on stratospheric ozone and global climate, Geophys. Res. Lett. 35 (2008) L19803, https://doi.org/10.1029/2008GL035102.

[23] W. Won, H. Kwon, J.-H. Han, J. Kim, Design and operation of renewable energy sources based hydrogen supply system: technology integration and optimization, Renew. Energy 103 (2017) 226–238.

[24] F. Barbir, PEM electrolysis for production of hydrogen from renewable energy sources, Sol. Energy 78 (2005) 661–669.

[25] E. Akyuz, C. Coskun, Z. Oktay, I. Dincer, Hydrogen production probability distributions for a PV-electrolyser system, Int. J. Hydrogen Energy 36 (2011) 11292–11299.

[26] C.R. Rodríguez, M. Riso, G. Jiménez Yob, R. Ottogalli, R. Santa Cruz, S. Aisa, et al., Analysis of the potential for hydrogen production in the province of Córdoba, Argentina, from wind resources, Int. J. Hydrogen Energy 35 (2010) 5952–5956.

[27] S.H. Siyal, D. Mentis, M. Howells, Economic analysis of standalone wind-powered hydrogen refueling stations for road transport at selected sites in Sweden, Int. J. Hydrogen Energy 40 (2015) 9855–9865.

[28] L. Viktorsson, J. Heinonen, J. Skulason, R. Unnthorsson, A step towards the hydrogen economy—a life cycle cost analysis of A hydrogen refueling station, Energies 10 (2017) 763.

[29] F. Posso, J. Sánchez, J.L. Espinoza, J. Siguencia, Preliminary estimation of electrolytic hydrogen production potential from renewable energies in Ecuador, Int. J. Hydrogen Energy 41 (2016) 2326–2344.

[30] Stephen Carr, Fan Zhang, Feng Liu, Zhaolong Du, Jon Maddy, Optimal operation of a hydrogen refuelling station combined with wind power in the electricity market, Int. J. Hydrogen Energy 41 (46) (2016) 21057–21066.

[31] L. Yang, M. He, V. Vittal, J. Zhang, Stochastic optimization-based economic dispatch and interruptible load management with increased wind penetration, IEEE Trans. Smart Grid 7 (2) (2016) 730–739.

[32] Morteza Zare Oskouei, Sadeghi Yazdankhah Ahmad, Scenario-based stochastic optimal operation of wind, photovoltaic, pump-storage hybrid system in frequency-based pricing, Energy Convers. Manag. 105 (2015) 1105–1114.

[33] Farhad Samadi Gazijahani, Sajad Najafi Ravadanegh, Javad Salehi, Stochastic multi-objective model for optimal energy exchange optimization of networked microgrids with presence of renewable generation under risk-based strategies, ISA (Instrum. Soc. Am.) Trans. 73 (2018) 100–111.

[34] R. Khodabakhsh, S. Sirouspour, Optimal control of energy storage in a microgrid by minimizing conditional value-at-risk, IEEE Trans. Sustain. Energy 7 (3) (2016) 1264–1273.

[35] X. Xu, W. Hu, D. Cao, W. Liu, Z. Chen, H. Lund, Implementation of repowering optimization for an existing photovoltaic-pumped hydro storage hybrid system: a case study in Sichuan, China, Int. J. Energy Res. (2019) 1–18.

[36] S. Nojavan, K. Zare, B. Mohammadi-Ivatloo, Application of fuel cell and electrolyzer as hydrogen energy storage system in energy management of electricity energy retailer in the presence of the renewable energy sources and plug-in electric vehicles, Energy Convers. Manag. 136 (2017) 404–417.

[37] C.H. Li, X.J. Zhu, G.Y. Cao, et al., Dynamic modeling and sizing optimization of stand-alone photovoltaic power systems using hybrid energy storage technology, Renew. Energy 34 (3) (2009) 815–826.

[38] Murat Gökçek, Cihangir Kale, Techno-economical evaluation of a hydrogen refuelling station powered by Wind-PV hybrid power system: a case study for İzmir-Çeşme, Int. J. Hydrogen Energy 43 (23) (2018) 10615–10625.

[39] Peng Hou, Peter Enevoldsen, Joshua Eichman, Weihao Hu, Mark Jacobson, Z. Chen, Optimizing investments in coupled offshore wind -electrolytic hydrogen storage systems in Denmark, J. Power Sources 359 (2017) 186–197.

[40] J. Alazemi, Automotive Solar Hydrogen Fuelling Stations: Concept Design, Performance Testing and Evaluation, RMIT University, 2016.

[41] B. Kruse, S. Grinna, C. Buch, Hydrogen: Status Og Muligheter, The Bellona Foundation, 2002.

[42] IEA, Hydrogen Production & Distribution, Energy Technology Essentials, 2007.

[43] M. Hamdan, PEM Electrolyzer Incorporating an Advanced Low Cost Membrane, 2012. https://www.hydrogen.energy.gov/pdfs/review12/pd030_hamdan_2012_o.pdf. (Accessed 1 November 2019).

[44] E. Dijoux, N.Y. Steiner, M. Benne, Marie-Cécile Péra, Brigitte Grondin Pérez, A review of fault tolerant control strategies applied to proton exchange membrane fuel cell systems, J. Power Sources 359 (2017) 119–133.

[45] Y. Li, W. Liu, M. Shahidehpour, F. Wen, K. Wang, Y. Huang, Optimal operation strategy for integrated natural gas generating unit and power-to-gas conversion facilities, IEEE Trans. Sustain. Energy 9 (4) (2018) 1870–1879.

[46] Mansour Hosseini-Firouz, Optimal offering strategy considering the risk management for wind power producers in electricity market, Int. J. Electr. Power Energy Syst. 49 (2013) 359–368.

[47] L. Wu, M. Shahidehpour, T. Li, Stochastic security-constrained unit commitment, IEEE Trans. Power Syst. 22 (2007) 800–811.

[48] Hai Lan, Shuli Wen, Ying-Yi Hong, David C. Yu, Lijun Zhang, Optimal sizing of hybrid PV/diesel/battery in ship power system, Appl. Energy 158 (2015) 26–34.

[49] F. Markert, S.K. Nielsen, J.L. Paulsen, V. Andersen, Safety aspects of future infrastructure scenarios with hydrogen refuelling stations, Int. J. Hydrogen Energy 32 (13) (2007) 2227–2234.